

# Collinear source of polarization-entangled photon pairs at non-degenerate wavelengths

P. Trojek and H. Weinfurter

*Department für Physik, Ludwig-Maximilians Universität, D-80799 München, Germany*

*Max-Planck-Institut für Quantenoptik, D-85748 Garching, Germany*

(Dated: January 12, 2008)

We report on a simple but highly efficient source of polarization-entangled photon pairs at non-degenerate wavelengths. The fully collinear configuration of the source enables very high coupling efficiency into a single optical mode and allows the use of long nonlinear crystals. With optimized dispersion compensation it is possible to use a free-running laser diode as pump source and to reach an entanglement fidelity of 99.4 % at rates as high as 27000 pairs/s per mW of pump power. This greatly enhances the practicality of the source for applications in quantum communication and metrology.

Entangled photons, for long time considered only as a tool for testing fundamental aspects of quantum theory [1], now become a basic building block for novel quantum communication and computation protocols, such as quantum cryptography [2], dense coding [3] or teleportation [4]. For the practical implementations, polarization encoding of photons is among the best choices due to the availability of reliable polarization-control elements and analyzers enabling high-fidelity measurements. To date, the most established way to generate entangled photon pairs is spontaneous parametric down-conversion (SPDC). In this process photons of an intense pump beam spontaneously convert in a second-order ( $\chi^{(2)}$ ) nonlinear crystal into two lower-frequency photons provided that energy and momentum is conserved. Two basic methods how to obtain polarization-entanglement from SPDC are widely applied: the first uses type-II phase-matching in a single crystal [5], and the second relies on the coherent spatial overlap of the emissions from two adjacent type-I phase-matched crystals [6]. Usually, due to the non-collinear geometry of the methods, the nonlinear crystal has to be relatively short (typically in range from 0.5 mm to 3 mm) and only a small fraction of the emitted SPDC flux can be collected, thereby limiting strongly the potential output brightness. Recently, a two-way collinear emission was employed inside a Sagnac interferometer to produce entangled photon pairs with long crystals or highly non-linear glass fibers [7]. This increases the output brightness significantly, but now requires interferometric alignment.

Here, we present a source of polarization-entangled photon pairs overcoming many deficiencies of the prior art, including those outlined above. We utilize the fact that photon pairs at non-degenerate wavelengths can be generated collinearly with respect to the pump light by SPDC and can thus be collected very efficiently into a single-mode fiber. The spectral information is then exploited to split the photons into two distinct spatial modes using a wavelength division multiplexer (WDM). This method produces polarization entanglement directly, without a need for any post-selection [8] or beam overlap [7], and can be used in all applications where the photons are observed separately.

For the actual generation of the photons, SPDC in the simple two-crystal geometry is applied [6]. Con-

sider two adjacent nonlinear crystals, both operated in type-I phase-matching configuration and pumped with linearly polarized light. The orientation of otherwise identical crystals is adjusted such that the optic axes of the first and second crystal lie in the vertical and horizontal planes, respectively. If the polarization of the pump beam is oriented under  $45^\circ$ , SPDC occurs equally likely in either crystal, producing pairs of horizontally- ( $|H\rangle|H\rangle$ ) or vertically-polarized ( $|V\rangle|V\rangle$ ) photons. By angle tuning the crystals, down-conversion is set to a collinear phase-matching configuration [9], emitting pairs of photons at non-degenerate wavelengths  $\lambda_1$  and  $\lambda_2$ . Provided that the two emission processes are coherent with one another, which is fulfilled as long as there is no way of ascertaining whether a photon pair was produced in the first or the second crystal, the entangled state  $|\phi(\varphi)\rangle = 1/\sqrt{2}(|H\rangle_{\lambda_1}|H\rangle_{\lambda_2} + e^{i\varphi}|V\rangle_{\lambda_1}|V\rangle_{\lambda_2})$  is produced.

In fact, dispersion and birefringence in the crystals lead to a partial loss of coherence between the two emission processes. Because the times, when the photons exit from the output face of the second crystal, depend on their wavelengths and polarizations, they potentially reveal the actual position of the photon-pair origin. This detrimental temporal effect is twofold, and can be better understood, when inspecting the dependence of the relative phase  $\varphi(\lambda_p, \lambda)$  on the wavelengths of pump ( $\lambda_p$ ) and one of the down-conversion photons, see Fig. 1(a). First, it is the group-velocity mismatch between the pump and the down-conversion light, which causes that the photon pairs born in the first crystal are advanced with regard to the pump photons and thus with regard to those originating in the second crystal. This manifests itself as a finite slope of the phase map  $\varphi(\lambda_p, \lambda)$  in the  $\lambda_p$  direction and it is usually precluded using narrowband pump [6]. To enable also the use of a broadband pump source, e.g., a free-running laser diode, here we use a special birefringent compensation crystal in the path of the pump, introducing a proper temporal retardation between its horizontally- and vertically-polarized components [9, 10], thus effectively pre-compensating the effect. Second, the dispersive delay between the down-conversion photons at the non-degenerate wavelengths is different for the two emission possibilities, because the photons generated in the first crystal acquire an extra spread when propagat-

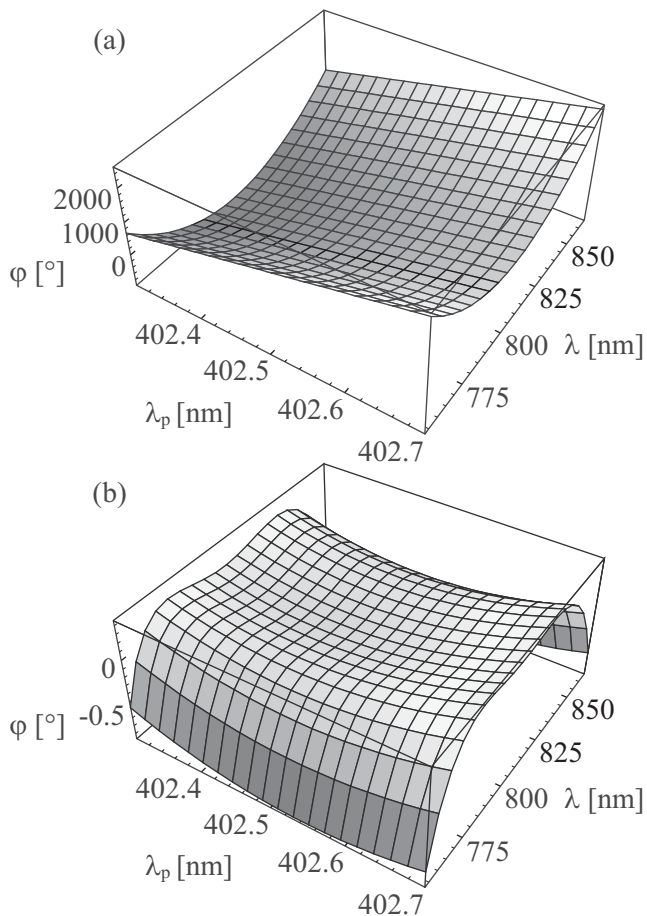


FIG. 1: Calculated dependence of the relative phase  $\varphi$  on the wavelengths of pump  $\lambda_p$  and one of the down-conversion photons  $\lambda$  for (a) uncompensated and (b) compensated configuration. The evaluation assumes SPDC in the pair of BBO crystals, each 15.76 mm thick and cut at  $\theta_p = 29.0^\circ$ ; an overall phase offset is suppressed for clarity. After the optimum compensation using a pair of tailored YVO<sub>4</sub> crystals with thicknesses of 8.20 and 9.03 mm, the phase surface is flat over the relevant spectral region (note the change in the vertical scale), indicating a high purity of the entangled state.

ing through the second crystal. As a consequence, the relative phase  $\varphi(\lambda_p, \lambda)$  varies strongly with the wavelength  $\lambda$  as well. An additional birefringent crystal with an effectively reverse phase characteristics has to be put behind the SPDC crystals to counteract this second effect. In this way, the initially strongly varying phase map  $\varphi(\lambda_p, \lambda)$  becomes flat [Fig. 1(b)], indicating the complete temporal indistinguishability of the emission processes. A more rigorous approach to the problem can be based on the evaluation of photon time distributions [11].

The setup of the source is schematically shown in Fig. 2. The linearly polarized pump light is provided by a 60 mW free-running laser diode operating at  $\lambda_p = 403$  nm ( $\Delta\lambda_p \approx 0.5$  nm). The light is reflected several times at UV-mirrors to remove the broadband background laser emission and passes through a half-wave plate rotating the polarization angle to  $45^\circ$ . Three lenses are used to correct the astigmatism of the laser diode

emission and to focus the pump beam to a diameter of  $\approx 220$   $\mu\text{m}$  within the two BBO ( $\beta\text{-BaB}_2\text{O}_4$ ) crystals (each  $6.0 \times 6.0 \times 15.76$  mm), both cut for type-I phase matching at  $\theta_p = 29.0^\circ$  and oriented for a collinear emission of photons at the wavelengths of  $\lambda_1 \approx 765$  nm and  $\lambda_2 \approx 850$  nm. The emitted photons are separated from the pump light using an IR-mirror and a longpass filter, and are collected into a single-mode fiber with an aspheric lens. To reach high collection efficiency, the lateral displacement of the horizontally and the vertically polarized photons caused by the birefringence of the BBO down-conversion crystals can be compensated best using the same pair of BBO crystals, but only half as long. The photons are directly guided to the custom made WDM, which splits the wavelengths  $\lambda_1$  and  $\lambda_2$  with a probability of over 99%. Labeling the spatial modes of the output single-mode fibers by 1 and 2, the polarization state of photons becomes  $|\phi(\varphi)\rangle = 1/\sqrt{2}(|H\rangle_1|H\rangle_2 + e^{i\varphi}|V\rangle_1|V\rangle_2)$ , provided that the two emission alternatives are temporally indistinguishable. This is achieved using two yttrium vanadate (YVO<sub>4</sub>) crystals, with their thicknesses  $d$  optimized according to the criteria described above. The first one ( $d = 8.20$  mm), is put into the path of the pump, whereas the other ( $d = 9.03$  mm) is included in the path of the down-conversion photons. Both YVO<sub>4</sub> crystals are cut at  $90^\circ$  with regard to pump- and fluorescence-light direction, in order to avoid spatial walk-off effects. For the detection of the down-conversion photons two actively quenched silicon avalanche photodiodes with

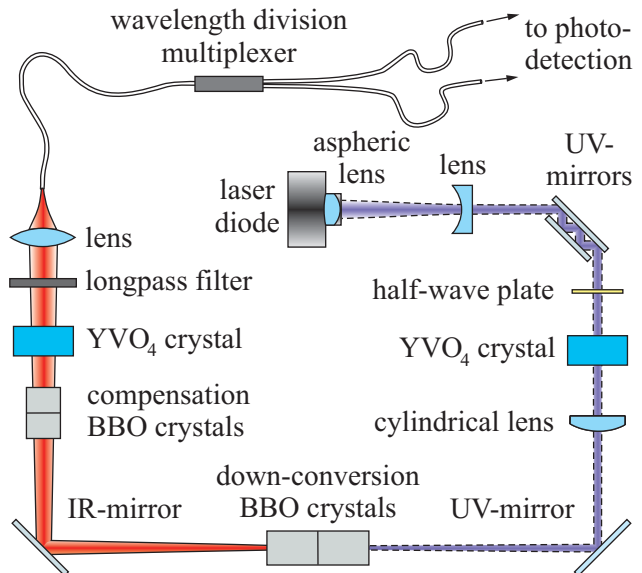


FIG. 2: Scheme of the collinear source. A free-running violet laser diode pumps a pair of BBO crystals and collinearly produces via SPDC pairs of non-degenerate photons, which are collected into a single mode fiber. The spectral information is exploited to separate the photons into two spatial modes using a wavelength division multiplexer. Two compensation YVO<sub>4</sub> crystals and BBO crystals are used to reverse the time delay effect and spatial lateral displacement effect, respectively, introduced in the down-conversion BBO crystals.

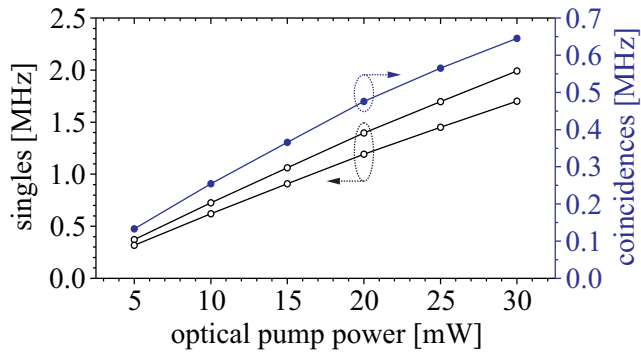


FIG. 3: Detected single and coincidence count rates depending on the pump power measured at the position of BBO crystals.

separately measured efficiency of 50–51 % at 800 nm were used.

With this source, we detected 27000 pairs per second and milliwatt of pump power (Fig. 3). Another important figure of merit, the coincidence-to-single ratio, reached values between 0.36 and 0.39 depending on the pump power, thereby confirming the very high coupling efficiency of photons into the single-mode fiber. Taking into account the limited detection efficiency and other losses in the set-up, such as the reflection at the fiber tips (all together > 12%) and the optics in the path of down-conversion photons (> 3%) or the insertion loss of the WDM (> 4%), we estimate the net coupling efficiency to reach values as high as 90%.

To verify the entanglement of photon pairs, the degree of polarization correlations in two complementary bases was measured using a pair of polarizers. At low pump power of  $\approx 1$  mW we obtained a visibility of  $V_{H/V} = 98.7 \pm 0.2\%$  in the horizontal/vertical basis and  $V_{45} = 98.4 \pm 0.3\%$  in the basis rotated by  $45^\circ$  or entanglement fidelity of  $F = 99.4\%$ , respectively. At higher pump powers the increased single photon rates, together with a relatively long coincidence gate time of  $\tau = 5.8$  ns, make correction for accidental coincidences necessary. The corrected visibilities are, within errors, consistent with those reported above. The gap between the measured value and the maximum visibility of 1 is attributed to depolarization inside the WDM.

The spectral distribution of the collected down-conversion photons was measured to be rather broad with the widths of  $\Delta\lambda_1 = 14.5 \pm 0.7$  nm and  $\Delta\lambda_2 = 15.4 \pm 1.2$  nm (Fig. 4). These values are in reasonable agreement with the theoretical values of  $\Delta\lambda_1 = 11.9$  nm and  $\Delta\lambda_2 = 12.9$  nm obtained for the actual parameters [11]. Substantially reduced widths of  $\Delta\lambda_1 = \Delta\lambda_2 = 6.4$  nm are expected for narrowband pumping.

Finally, we note that in the current realization we could not take the expected advantage of higher photon-pair fluxes converted in long down-conversion crystals. The additional measurements with BBO crystals of lengths  $L = 3.94$  mm and  $L = 7.88$  mm reveal only a negligible growth of the detected photon-pair rate  $\propto L^{0.1}$ . This dependence is considerably slower than that inferred theoretically [12],  $\propto \sqrt{L}$ ; (for

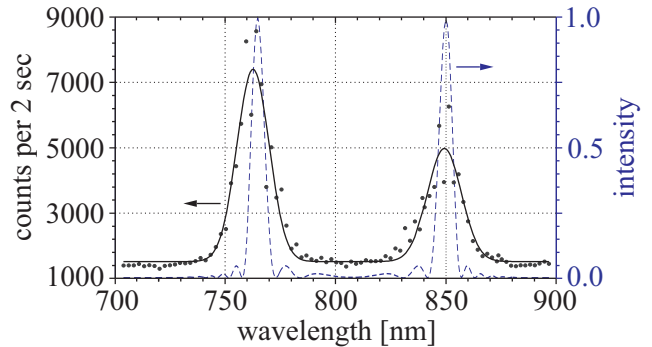


FIG. 4: Spectral distribution of down-conversion light with the central wavelengths of  $\lambda_1 = 762.8 \pm 0.4$  nm and  $\lambda_2 = 849.4 \pm 0.6$  nm, determined from a Gaussian fit (solid line). The lower peak number of counts at  $\lambda_2$  is due to a reduced efficiency of the spectrometer (with resolution 1.2 nm) towards infrared wavelengths. The dashed line shows the numerically simulated spectra obtained under the assumption of narrowband pumping.

the scaling of the down-conversion bandwidth with  $L$ , there is a good agreement between the experiment,  $\Delta\lambda \propto L^{-0.68}$ , and the theory,  $\Delta\lambda \propto L^{-0.73}$ ). We attribute the observed discrepancy to the two-crystal geometry, which does not allow the optimum simultaneous coupling of photons from both crystals, and to the spatial walk-off effect in the birefringent BBO crystals resulting in a spatial asymmetry of the down-conversion emission.

In summary, the fully collinear configuration of the source utilizing only one spatial mode for collecting down-conversion photons enables unprecedented coupling efficiencies and brings many more advantages. First, it minimizes the complexity of the source and thereby enhances its inherent robustness. Second, it precludes the occurrence of any intrinsic spatial effect limiting the quantum-interference visibility, while at the same time allows the use of long down-conversion crystals yielding higher photon-pair rates. From a practical point of view, the technical requirements and the demand for alignment are enormously reduced. These advantages make the source ideal for applications like quantum cryptography [2], multiparty single qubit communication [13] and single photon detector calibration [14]. The already high brightness reported here can be further improved with periodically poled crystals, allowing to noncritically phase match any set of wavelengths and thus avoid the spatial walk-off effects. In addition, it becomes possible to access the largest nonlinear coefficients, which in turn suggests that an increase of photon-pair rates by 1–2 orders of magnitude should be certainly feasible in the future.

The authors thank Y. Nazirizadeh for his assistance in the early stages of the project. This work was supported by Deutsche Forschungsgemeinschaft through the DFG-Cluster of Excellence MAP, by the DAAD-PPP Croatia program, and by the European Commission through the EU projects QAP and SECOQC.

- 
- [1] S. J. Freedman and J. F. Clauser, *Phys. Rev. Lett.* **28**, 938 (1972); L. Mandel, *Rev. Mod. Phys.* **71**, S274, (1999); A. Zeilinger, *Rev. Mod. Phys.* **71**, S288, (1999).
- [2] A. K. Ekert, *Phys. Rev. Lett.* **67**, 661 (1991); C. H. Bennett, G. Brassard, and N. D. Mermin, *Phys. Rev. Lett.* **68**, 557 (1992).
- [3] C. H. Bennett and S. J. Wiesner, *Phys. Rev. Lett.* **69**, 2881 (1992).
- [4] C. H. Bennett, G. Brassard, C. Crépeau, R. Jozsa, A. Peres, and W. K. Wootters, *Phys. Rev. Lett.* **70**, 1895 (1993).
- [5] P. G. Kwiat, K. Mattle, H. Weinfurter, A. Zeilinger, A. V. Sergienko, and Y. Shih, *Phys. Rev. Lett.* **75**, 4337 (1995).
- [6] P. G. Kwiat, E. Waks, A. G. White, I. Appelbaum, and P. H. Eberhard, *Phys. Rev. A* **60**, R773 (1999).
- [7] F. N. C. Wong, J. H. Shapiro, and T. Kim, *Laser Physics* **16**, 1517 (2006); X. Li, P. L. Voss, J. E. Sharping, and P. Kumar, *Phys. Rev. Lett.* **94**, 053601 (2005); J. Fulconis, O. Alibart, J. L. O'Brien, W. J. Wadsworth, and J. G. Rarity, *Phys. Rev. Lett.* **99**, 120501 (2007); J. Fan, M. D. Eisaman, and A. Migdall, *Phys. Rev. A* **76**, 043836 (2007).
- [8] T. E. Kiess, Y. H. Shih, A. V. Sergienko, and C. O. Alley, *Phys. Rev. Lett.* **71**, 3893 (1993).
- [9] Y.-H. Kim, S. P. Kulik, and Y. Shih, *Phys. Rev. A* **63**, 060301 (2001).
- [10] Y. Nambu, K. Usami, Y. Tsuda, K. Matsumoto, and K. Nakamura, *Phys. Rev. A* **66**, 033816 (2002).
- [11] P. Trojek, Ph. D. thesis, LMU München (2007).
- [12] D. Ljunggren and M. Tengner, *Phys. Rev. A* **72**, 062301 (2005).
- [13] C. Schmid, P. Trojek, M. Bourennane, C. Kurtsiefer, M. Żukowski, and H. Weinfurter, *Phys. Rev. Lett.* **95**, 230505 (2005); Z. J. Zhang, Y. Li, and Z. X. Man, *Phys. Rev. A* **71**, 044301 (2005); P. Trojek, C. Schmid, M. Bourennane, Č. Brukner, M. Żukowski, and H. Weinfurter, *Phys. Rev. A* **72**, 050305 (2005).
- [14] D. N. Klyshko, *Sov. J. Quantum Electron.* **10**, 1112 (1980); J. G. Rarity, K. D. Ridley, and P. R. Tapster, *Appl. Opt.* **26**, 4616 (1987).